

Trajectory fluctuations accompanying the manipulation of spherical nanoparticles

Akshata Rao,¹ Marie-Luise Wille,¹ Enrico Gnecco,¹ Karine Mougín,² and Ernst Meyer¹¹*Department of Physics, University of Basel, Klingelbergstrasse 82, 4056 Basel, Switzerland*²*ICSI-CNRS, 15 Rue Jean Starcky, 68057 Mulhouse, France*

(Received 30 July 2009; revised manuscript received 30 September 2009; published 10 November 2009)

We relate the frictional forces acting on spherical nanoparticles pushed by a scanning probe tip on a flat surface to the trajectories of the particles. Based on a simple collisional model, we predict that the average direction of motion of the nanoparticles is almost independent of the friction force, whereas the fluctuations of the particle directions are inversely proportional to friction. The model is applied to interpret the trajectory fluctuations and the apparent discontinuities observed when spherical gold particles are manipulated on a silicon-oxide surface by atomic force microscopy.

DOI: [10.1103/PhysRevB.80.193405](https://doi.org/10.1103/PhysRevB.80.193405)

PACS number(s): 68.37.Ps

I. INTRODUCTION

Controlling the trajectory of a nanoparticle sliding on a solid surface is extremely important in applications ranging from drug delivery to environmental control. Atomic force microscopy (AFM) has proven to be an ideal tool to manipulate single nanoparticles. Although important results have been achieved by AFM in contact mode,^{1,2} manipulation can be better controlled when the microscope is operated in tapping mode.³⁻⁵ In such a case the probing tip oscillates at a certain frequency close to the resonance of the free cantilever support and, provided that the oscillation amplitude is high enough, the tip can push nanoparticles on a substrate. In tapping mode AFM, the power dissipation P accompanying the particle motion can be quantified from the phase shift between the cantilever oscillations and the excitation signal.⁶ If the particles are displaced by a quantity d at each collision with the tip, the friction force f is in the order of $P/\omega d$. Assuming that the distance d corresponds to the lattice constant a of the substrate, Ritter *et al.*⁴ estimated a shear stress of some hundreds of MPa in the case of antimony particles sliding on graphite and molybdenum disulfide. The assumption $d=a$ was somehow supported by measurements of atomic-scale friction, where nanotips pulled on crystal surfaces (without particles) usually undergo a stick-slip motion with the periodicity of the surface lattice.⁷ However, it is questionable whether nanoparticles, pushed by a vibrating tip, should behave in the same way as a sharp tip sliding on a surface.

In this Brief Report, we proposed a different approach which allow us to precisely determine the mean displacement d of spherical nanoparticles moved by an AFM tip in tapping mode. The trajectories of the nanoparticles are reproduced by computer simulations, and we show that the fluctuations of the trajectories (but not their average directions) are significantly affected by friction. The larger the friction force f between particles and surface, the more regular the trajectories. In case of very large friction, our results are well reproduced by an analytical formula, which we have introduced in a recent work.⁵ Without knowing the friction force, the mean distance d traveled by the particles after a collision can be simply estimated from the fluctuations observed in the AFM measurements.

II. MODEL

We assume that the AFM is operated in tapping mode, and that the oscillation amplitude of the tip is large enough to set the nanoparticles into motion.⁸ Due to the finite friction force f , a particle is displaced of a quantity d at each collision with the tip apex. Assuming that the particle slides without rolling,⁹ the displacement d is simply related to the kinetic energy E_{kin} acquired by the particle by the relation

$$d = \frac{E_{\text{kin}}}{f} = \frac{mv^2}{2f},$$

where m is the particle mass and v is the velocity of the particle immediately after the collision with the tip. Depending on the value of d , the oscillation frequency ω of the cantilever, the scan velocity v_s , and the tip and particle sizes, the particle will experience a certain number of collisions along each scan line, varying between zero and $\sim \omega R/v_s$, where R is the sum of the radii of the tip and particle sections taken at the contacting point. If the particle radius $R_p < R_t(1 - \sin \gamma)$, where R_t is the tip radius and γ is the semia-perture angle of the tip cone, the quantity R is twice the geometric average of tip and particle radii: $R = 2\sqrt{R_p R_t}$. Otherwise, a more complicated relation holds, as described in Ref. 5.

In the following, we simulate the particle trajectories in two dimensions, and consider the sections of tip and particle at their point of contact. On the first scan line, the particle is positioned such as its distance from the scan line takes a random value between 0 and R . The tip moves forth and back along the x axis, and it is shifted of a quantity b along the y direction at the end of each scan. At every collision with the tip, the particle is displaced of a quantity d along the straight line joining the centers of tip and particle. Figure 1 shows two trajectories corresponding to different values of the parameter d . For the spacing between consecutive scan lines we have chosen a typical value $b = 15$ nm. If $d \ll b$ the particle trajectory is quite regular, except for the first scan line, where the tip touches the particle at an arbitrary angle [Fig. 1(a)]. However, the situation changes when d is on the order of b or larger. In such a case, the particle trajectory fluctuates and apparent discontinuities, i.e., scan lines with-

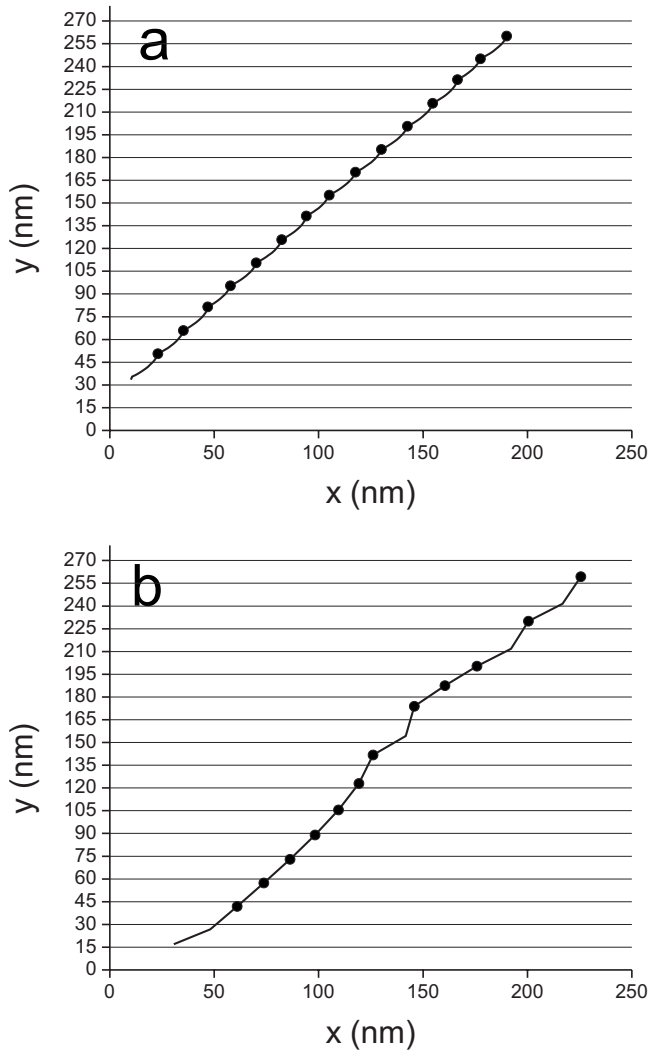


FIG. 1. Simulated trajectories of a nanosphere pushed by an AFM tip in tapping mode. The center of the tip follows the horizontal lines, which are separated by a distance $b=15$ nm. The sum of the radii of the sections of tip and particle (at their contact point) is $R=35$ nm and the displacement of the particle after collision is (a) $d=2$ nm and (b) 20 nm. The black dots represent the particle position at the end of each scan line.

out collisions between tip and particles, can be observed [Fig. 1(b)].

Figure 2(a) shows the average slope of the particle trajectory as a function of the displacement d (with the same values of R and b used in Fig. 1). With our choice of parameters, the average value of the deflection angle, $\bar{\theta}$, takes always a value of about 52° , except in the range $b \sim d$. We have also calculated the fluctuations of the particle direction from the straight line defined by $\bar{\theta}$. In Fig. 2(b) the fluctuations are defined by the root mean square δs of the distance between the points forming the trajectory and the straight line. The quantity δs is plotted as a function of the displacement d . In contrast to the average direction $\bar{\theta}$, the fluctuations δs present a strong dependence on d . As shown in Fig. 2(b), the fluctuations δs are proportional to the displacement d in the range of values considered in the simulation (up to

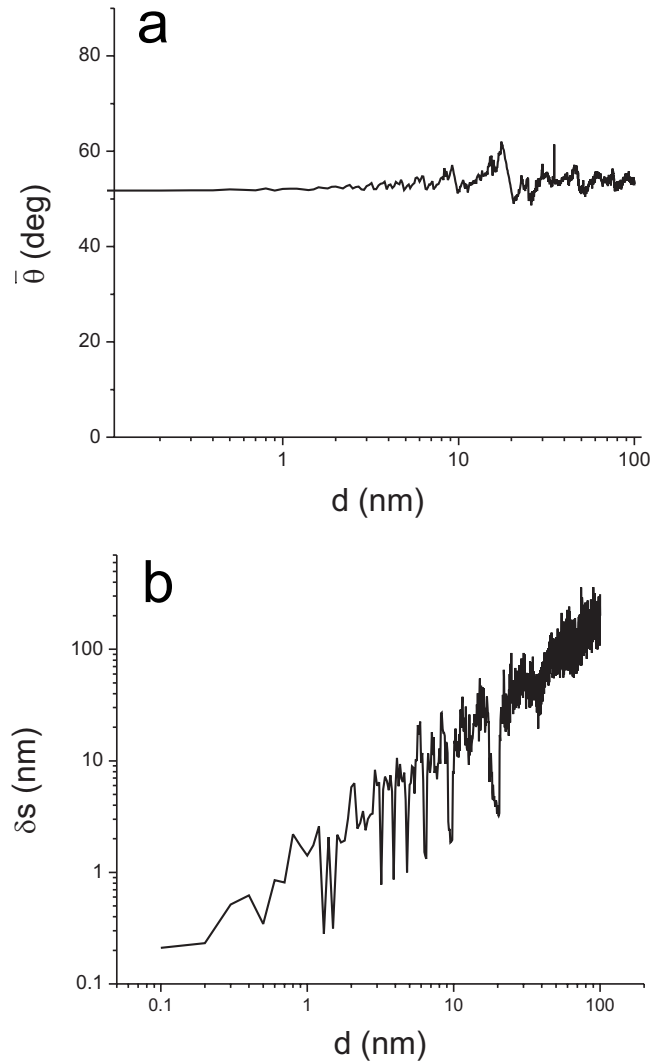


FIG. 2. (a) Average angle of deflection and (b) fluctuations of the trajectories of spherical particles plotted as a function of the “mean path” d of the nanoparticles. The parameters R and b have the same values as in Fig. 1.

$d=100$ nm). From a fit of the curve shown in Fig. 2(b) it turns out that $\delta s \approx d$. However, this is not the case in a few isolated dips and in the region $d \sim b$, where the fluctuations are significantly smaller.

III. EXPERIMENTAL RESULTS AND DISCUSSION

The angle of deflection of a spherical particle has been calculated in Ref. 5 assuming that the adhesion between substrate and particles is strong enough to prevent any further displacement of the particle after the collision with the tip. In such case, corresponding to the limit $d \rightarrow 0$, we showed that

$$\tan \theta = - \frac{b}{R \left(\cos \alpha_0 + \log \tan \frac{\alpha_0}{2} \right)}, \quad (1)$$

where α_0 is the impact angle between tip and particle. For a raster scan path the impact angle is

$$\alpha_0 = \arcsin\left(1 - \frac{b}{R}\right), \quad (2)$$

except for the very first scan line.

The results in Fig. 2(a) show that the average deflection of the particle does not change by increasing d , except in the region $d \sim b$. We can explain this result as follows. When $d \rightarrow 0$ the particle and tip meet each other at the same relative position, defined by the impact angle α_0 , in every scan line except the first one. By increasing d the impact angle is different in every scan line. Depending on b , angles below and above α_0 are expected. As it turns out from our numeric results, the distribution of the impact angles around α_0 is well balanced, except when $d \sim b$. Other simulations (not shown here) have showed that, when $b \ll R$ significant deviations are observed if $d = nb$ or b/n , where n is a small integer number. In such a case, the tip and particle will meet each other at an angle $> \alpha_0$, which is approximately the same in every consecutive line. When $b \sim R$, as in Fig. 2, this “interference” effect is still present, although it is significantly smoothed out.

In order to test our model and to estimate the parameter d in real cases, we have manipulated gold nanoparticles with 50 nm diameter (PGO-50, G. Kisker GbR, Germany) on flat silicon wafers. Since the experiment was carried under ambient conditions (RH 40%), the substrate was covered by a thin layer of amorphous silicon oxide (with an average thickness of 1.5 nm, as estimated by ellipsometry measurements). A commercial AFM (Nanite™, Nanosurf AG, Switzerland) operated in tapping mode has been used for manipulation experiments. The path of the nanoparticles is clearly revealed in the forward traces of the topography signal [Fig. 3(a)]. In Fig. 3(a) the nanoparticles have an apparent height of 30–35 nm, indicating that they are displaced before the tip reaches the top of the particles. When the tip is scanned backward, the mobile particles do not appear at all [Fig. 3(b)], meaning that they are completely pushed away from the scan “corridor” when the tip moves forward. The mean angle of deviation $\bar{\theta}$ of the three particles in Fig. 3 is 62° and their trajectory fluctuations δs are 19.5, 22.8, and 20.4 nm, respectively. From the value of $\bar{\theta}$ (with $b = 7.8$ nm), we estimate $R = 64$ nm using Eqs. (1) and (2), and from simulations with these values of δs and R , we estimate a value $d = 20$ nm for the mean displacement of the particles. This value is much higher than the lattice constant of the substrate (~ 0.5 nm). However, when the contact area is extended over several unit cells, it is well established that friction may be significantly lowered by incommensurability effects,¹⁰ resulting in a longer jump length. This possibility has to be taken into account in our case, since silicon oxide has an amorphous structure and the gold particles are possibly covered by a residual layer of surfactant (such as sodium citrate), which change the chemical interaction with the substrate. On commensurate contacts of similar size the effect of friction reduction does not appear and the jump length may remain in the order of the lattice constant, as commonly observed in the sliding of atomically sharp tips.⁷

Several discontinuities can also be noticed in the particle trajectories. The exact condition for the appearance of a dis-

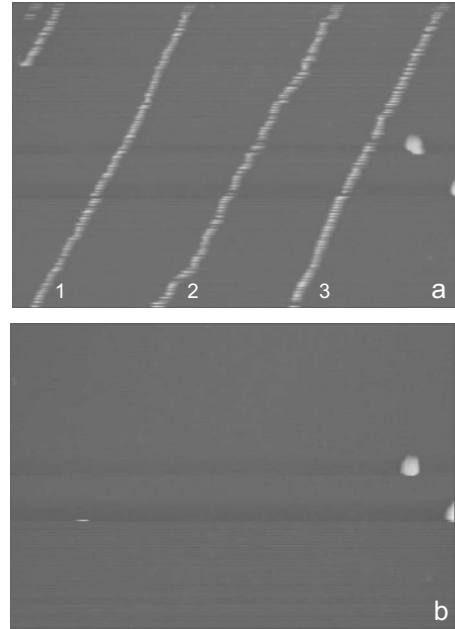


FIG. 3. (a) Forward and (b) backward topography images showing the trajectories of gold nanospheres pushed by an AFM tip on a silicon surface in tapping mode (frames size: $3.85 \times 2.65 \mu\text{m}^2$). The particles have a radius of 25 nm and the distance between consecutive scan lines is $b = 7.8$ nm.

continuity is $D(i) = [y_{i+1}/b] - [y_i/b] > 1$, where i enumerates the collisions between tip and nanoparticles and the square bracket denotes the integer part of a real number. In Fig. 4 the histograms of the functions $D(i)$ corresponding to the three particles in Fig. 3(a) are shown. The average values of the discontinuities are 17.6, 26.5, and 18.8 nm, respectively, i.e., in the same range of the displacement d . From numeric simulations with $d = 20$ nm, $R = 64$ nm, and $b = 7.8$ nm we obtain a value 15.6 nm for the average discontinuity. Although measuring the apparent discontinuities in the particles

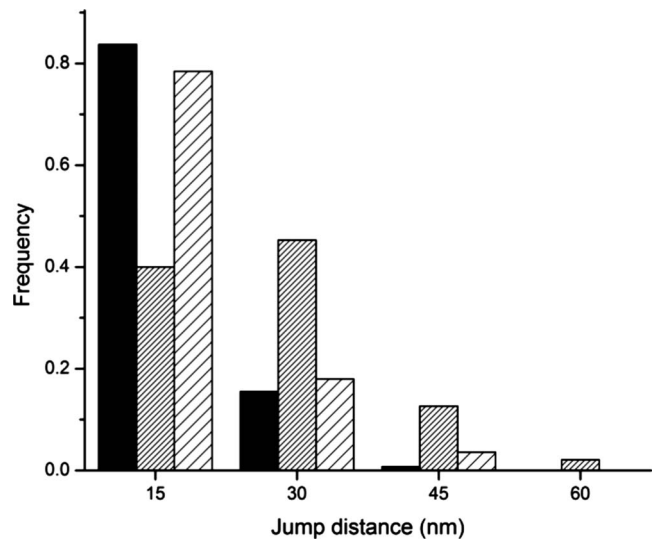


FIG. 4. Statistic distribution of the discontinuities in the trajectories of the three particles enhanced in Fig. 4(a). The average value of the discontinuities is 20.6 nm.

trajectories may represent an easier way to evaluate the mean displacement of the nanoparticles after collision, the discretization in the y direction makes this procedure less reliable than measuring the fluctuations of the particle trajectories.

IV. CONCLUSIONS

In conclusion, we have theoretically investigated how friction affects the trajectories of spherical nanoparticles pushed by an AFM tip on a flat surface. Our model has been applied to determine the mean displacement of gold particles on silicon oxide in air. This quantity turned out to be significantly larger than the lattice constant of the substrate, as assumed in previous works on the topic. Since the velocities of the particles immediately after a collision are unknown, the friction force between particles and surface could not be quantified. This drawback may be overcome once the collision process between tip and particle is better understood, for instance, by measuring the amplitude variations in the cantilever oscillations in real time and/or modeling the tip-particle interactions by combinations of molecular dynamics and continuum mechanics.

A comment has also to be made concerning the assumption that the particles slide without rolling. Ritter *et al.*⁹ showed that this hypothesis is valid in the case of latex nano-

spheres (with radii of a few tens of nm) manipulated on highly oriented pyrolytic graphite after the orientation of the spheres had been marked by slight indentations made by the AFM tip. Unfortunately, this cannot be done on gold nanoparticles. Furthermore, smaller objects such as C_{60} molecules were reported to roll in scanning tunnel microscope manipulation experiments on Si(100).¹¹ Ongoing theoretical works on spherical clusters have shown that both sliding and rolling regimes are expected, depending on a delicate balance between the model parameters.^{12,13} Manipulation experiments on particles with different shapes may help to shed light into this puzzling question. Apart from the shape of the nanoparticles, surface and environmental properties such as roughness,¹⁴ humidity,¹⁵ and chemical functionalization⁸ play an important role in manipulation experiments at room temperature. For instance, a moderate adhesion between tip and particle may increase the value of the parameter d . Altogether, these effects must be taken into account in future extensions of our model.

ACKNOWLEDGMENTS

The Swiss National Center of Competence in Research on Nanoscale Science, the National Science Foundation, and the European Science Foundation EUROCORES Programme FANAS are gratefully acknowledged for financial support.

¹R. Lüthi, E. Meyer, H. Haefke, L. Howald, W. Gutmannsbauer, and H.-J. Güntherodt, *Science* **266**, 1979 (1994).

²D. Dietzel, C. Ritter, T. Mönninghoff, H. Fuchs, A. Schirmeisen, and U. D. Schwarz, *Phys. Rev. Lett.* **101**, 125505 (2008).

³R. Resch, D. Lewis, S. Meltzer, N. Montoya, B. E. Koel, A. Madhukar, A. A. G. Requicha, and P. Will, *Ultramicroscopy* **82**, 135 (2000).

⁴C. Ritter, M. Heyde, B. Stegemann, K. Rademann, and U. D. Schwarz, *Phys. Rev. B* **71**, 085405 (2005).

⁵A. Rao, E. Gnecco, D. Marchetto, K. Mougín, M. Schönenberger, S. Valeri, and E. Meyer, *Nanotechnology* **20**, 115706 (2009).

⁶R. Garcia, J. Tamayo, and A. San Paulo, *Surf. Interface Anal.* **27**, 312 (1999).

⁷E. Gnecco, R. Bennewitz, T. Gyalog, Ch. Loppacher, M. Bammerlin, E. Meyer, and H.-J. Güntherodt, *Phys. Rev. Lett.* **84**, 1172 (2000).

⁸K. Mougín, E. Gnecco, A. Rao, M. T. Cuberes, S. Jayaraman, E. W. McFarland, H. Haidara, and E. Meyer, *Langmuir* **24**, 1577 (2008).

⁹C. Ritter, M. Heyde, U. D. Schwarz, and K. Rademann, *Langmuir* **18**, 7798 (2002).

¹⁰M. Dienwiebel, G. S. Verhoeven, N. Pradeep, J. W. M. Frenken, J. A. Heimberg, and H. W. Zandbergen, *Phys. Rev. Lett.* **92**, 126101 (2004).

¹¹N. Martsinovich, C. Hobbs, L. Kantorovich, R. H. J. Fawcett, M. J. Humphry, D. L. Keeling, and P. H. Beton, *Phys. Rev. B* **74**, 085304 (2006).

¹²M. Evstigneev (private communication).

¹³M. H. Korayem and M. Zakeri, *Int. J. Adv. Manuf. Technol.* **41**, 714 (2009).

¹⁴M. Götzinger and W. Peukert, *Langmuir* **20**, 5298 (2004).

¹⁵M. Palacio and B. Bhushan, *Nanotechnology* **19**, 315710 (2008).